Raman study of oxygen in the oxide superconductor $Bi_2CaSr_2Cu_2O_{8+\delta}$

Y. H. Shi
Department of Physics and Department of Chemistry, University of Toronto, Toronto, Ontario, Canada

M. J. G. Lee
Department of Physics and Scarborough College, University of Toronto, Toronto, Ontario, Canada

M. Moskovits
Department of Chemistry, University of Toronto, Toronto, Ontario, Canada

R. Carpick, A. Hsu, B. W. Statt, and Z. Wang
Department of Physics, University of Toronto, Toronto, Ontario, Canada

(Received 10 May 1991)

The zero-resistance temperature of the high-T_c oxide superconductor $Bi_2CaSr_2Cu_2O_{8+\delta}$ (2:1:2:2) can be significantly increased by annealing at 500 °C in an oxygen-reduced environment. Raman spectroscopy of high-density sintered samples shows that processing the material in this way increases the strength of the Raman peak of highest frequency (650 cm^{-1}), leaving the strengths of the other oxygen peaks unchanged. The Raman data confirm that the mobile oxygen atoms are located in the bismuth layer and support those models of oxygen structure in which excess oxygen is incorporated interstitially. They provide evidence that the incommensurate-to-commensurate transition observed in electron diffraction in the vicinity of 500 °C is associated with a loss of oxygen from the bismuth layer.

I. INTRODUCTION

Since the discovery of the bismuth-based cuprate superconductors by Maeda *et al.*,[1] several superconducting phases have been reported in the Bi-Ca-Sr-Cu oxide system. Among them, a phase with a transition temperature in the vicinity of 10 K has been identified as $Bi_2Sr_2CuO_{6+\delta}$ (2:0:2:1), an 84-K phase has been identified as $Bi_2CaSr_2Cu_2O_{8+\delta}$ (2:1:2:2), and a 108-K phase has been identified as $Bi_2Ca_2Sr_2Cu_3O_{10+\delta}$ (2:2:2:3). These compounds are all layered oxygen-deficient perovskites.[2] Sample preparation conditions, such as the annealing temperature, annealing time, cooling rate, and ambient gas, can influence the superconducting properties of the Bi-Sr-Ca-Cu oxide superconductors, apparently by varying δ, the degree of oxygenation.

From various studies of x-ray-diffraction and neutron diffraction in bismuth 2:1:2:2, a consistent picture of the average structure of the cations has emerged. The structure is orthorhombic, with calcium, copper, strontium, and bismuth atoms confined to separate layers. Neutron-diffraction data showed that there is no oxygen in the calcium layer, while metal and oxygen atoms alternate in the copper and strontium layers.[3] Early neutron-diffraction data were interpreted as indicating that oxygen is incorporated by the progressive occupation of the vacant sites in a BiO layer until a commensurate BiO_2 structure is reached.[4–7] More recently, high-resolution electron microscopy data[8,9] have shown that at room temperature the oxygen structure in the bismuth layer is incommensurate, and the existence of an oxygen superlattice in the bismuth layer has been confirmed by neutron diffraction.[10] Electron-diffraction data have shown that a transition from a low-temperature incommensurate phase to a high-temperature commensurate phase occurs in the vicinity of 500 °C.[11,12] The goal of this work is to seek evidence to link these observations by studying changes in the oxygen peaks in the Raman spectrum of bismuth 2:1:2:2 in the temperature range from room temperature to close to the melting point.

Each peak in the vibrational Raman spectrum corresponds to the motions of groups of atoms along the normal coordinate. Lattice dynamical calculations of the Raman and infrared (IR) active vibrational modes of $Bi_2CaSr_2Cu_2O_8$ have been carried out by Prade *et al.*[13] based on a simplified unit cell proposed by Tarascon *et al.*[14] While the calculated frequencies of the Raman modes depend to some extent on assumptions about the superlattice and the interatomic potentials, the ordering of the modes in frequency and the amplitudes of the associated atomic vibrations are determined almost exclusively by the local symmetry of the structure. It is found that, relative to the copper-oxygen angle-bending modes, the peaks at lower Raman shifts correspond to normal modes that are dominated by vibrations of the cations, while peaks at higher Raman shifts correspond to normal modes that are dominated by vibrations of oxygen atoms in the strontium and bismuth layers.

In the various experimental studies of the Raman spectra of the oxide superconductors reported to date, only Raman-active modes polarized normal to the *ab* planes have been detected. The electrical conductivity of these materials is highly anisotropic. Presumably the in-plane component of the electric field of the illuminating beam is

strongly attenuated because the conductivity parallel to the *ab* planes is high. The various peaks have been assigned to vibrational modes of the lattice on the basis of symmetry arguments, the results of lattice dynamical calculations, and comparisons with the Raman spectra of related materials. By studying the polarization dependence of the Raman spectrum of a single crystal, Cardona *et al.*,[15] demonstrated that the out-of-phase angle-bending (B_{1g}) vibrational mode of the oxygen atoms in the CuO layers occurs in the grouping near 300 cm^{-1}. Since this mode and the corresponding in-phase A_{1g} mode of oxygen atoms in the CuO layer are not expected Since this mode and the corresponding in-phase A_{1g} mode of oxygen atoms in the CuO layer are not expected to differ greatly in frequency, the A_{1g} mode is also assigned to this grouping. The softening observed below the superconducting transition has led Boekholt *et al.* to assign the peak near 470 cm^{-1} to in-phase vibrations of oxygen in the copper layer.[15a] The peak near 650 cm^{-1} is generally attributed to the A_{1g} vibrations of the oxygen atoms in the bismuth layer.

The intensities of the various vibrational Raman peaks are a measure of the modulation of the dielectric function of the sample that accompanies the vibration of the lattice in its various normal modes. The modulation of the dielectric function, which comes about through modulation of the electron density, is dominated by the motion of the lightest atoms, which in these structures are the oxygen atoms.

Laser annealing in a Raman spectrometer, in which the illuminating laser beam serves the dual role of heating the sample and exciting the Raman spectrum, proves to be a practical technique for studying oxygen effects in the oxide superconductors. The temperature rise, which is highly localized but essentially uniform over the illuminated area, can be determined by measuring the strengths of corresponding peaks in the Stokes and anti-Stokes spectra.[16] The intensities of the oxygen peaks in the Raman spectrum prove to be highly sensitive to changes in the distribution of the light oxygen atoms.

This paper reports a Raman spectroscopic study of the effect of laser annealing between room temperature and the melting temperature on the oxygen content of the various layers of the bismuth 2:1:2:2 oxide superconductor. Our samples are high-density, high-purity, sintered materials. Their Raman spectra show prominent peaks that are attributable to normal modes of the lattice that are dominated by motions of the oxygen atoms in the copper, strontium, and bismuth layers. Annealing in an oxygen-reduced atmosphere within a narrow temperature range close to 500 °C is found to cause an irreversible increase in the strength of the peak that corresponds to oxygen in the bismuth layer. The implications of the Raman data for the oxygen structure of bismuth 2:1:2:2 are discussed.

II. SAMPLE PREPARATION AND CHARACTERIZATION

Samples were prepared by a conventional solid-state reaction technique, starting from BaO, $SrCO_3$, $CaCO_3$, and CuO, each of purity 99.995%. The nominal composition is $Bi_2CaSr_2Cu_2O_{8+\delta}$. The starting materials were machine ground for 2 h, then calcined at 800 °C for 12 h. The calcined powders were reground for 2 h and then sintered at 870 °C for 24 h. The sintered materials were reground for 2 h, pelletized, annealed in air for 80 h at 860 °C, and furnace cooled at room temperature.

The samples prepared in this way were annealed at 500 °C for 24 h in a flow of dry nitrogen gas, and then furnace cooled. The temperature dependence of the ac susceptibility was measured down to 78 K. Results for a typical sample are shown in Fig. 1. The plot of susceptibility against temperature has a plateau extending from 83 to 94 K, indicating the presence of two superconducting phases, which are believed to be associated with oxygen inhomogenity within the grains of the polycrystalline sample.

Electrical resistivity was measured by a four-terminal technique with a current of 10 mA, using silver paste to make the electrical contacts. Curve (a) in Fig. 2 shows the resistance of a typical sample plotted as a function of temperature. Our various samples exhibit zero-resistance temperatures in the range 90 to 94 K, which is significantly higher than the 84 K that is usually considered to be the zero-resistance temperature of the 2:1:2:2 phase of the Bi-Ca-Sr-Cu oxide system, and in line with the enhanced zero-resistance temperatures reported in samples prepared under low partial pressures of oxygen,[17] with the T_c of 95 K reported for argon-annealed sintered samples,[18] and for samples prepared from citrate precursors.[19]

Our samples were then annealed again at 500 °C for 24 h, but this time in a flow of dry oxygen gas. The ac sus-

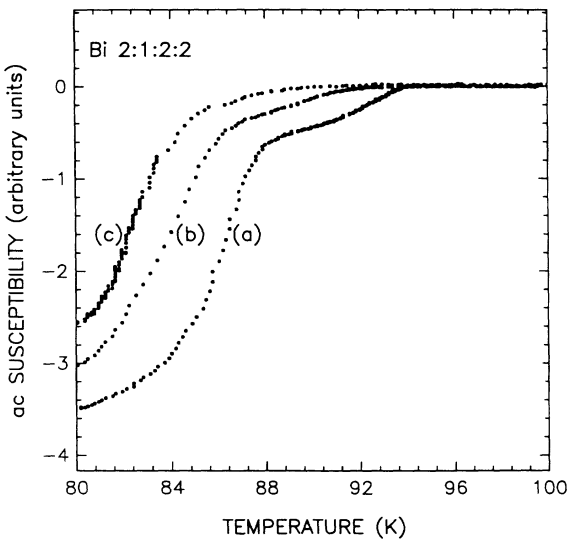

FIG. 1. ac susceptibility of a sample prepared by annealing for 24 h at 500 °C in an atmosphere of dry nitrogen gas. (a) susceptibility in zero magnetic field, (b) the effect of applying a static magnetic field of 80 G, and (c) the effect of applying a static magnetic field of 150 G. The data indicate the presence of two distinct phases, which are believed to differ only in oxygen structure.

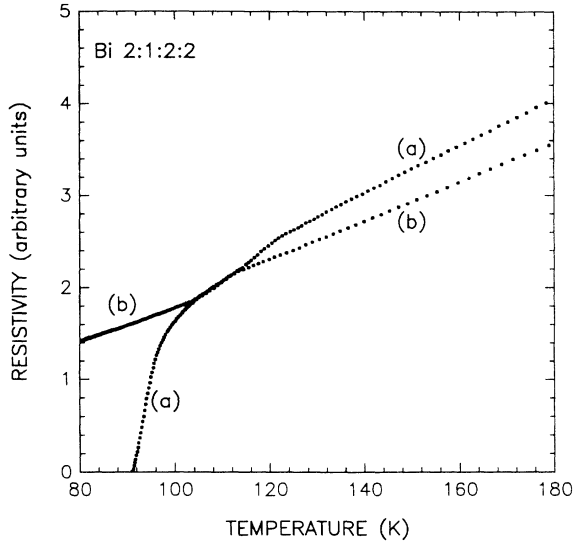

FIG. 2. dc resistivity of a sample prepared by annealing under (a) dry nitrogen and (b) dry oxygen gas at 500 °C. The zero-resistance temperature of the nitrogen-annealed sample is 91 K. As the silver paste contacts were replaced between measurements, the data have been scaled to match just above the onset of the superconducting transition. The weak anomalies at higher temperature are thought to indicate the presence of a small fraction of higher-T_c phase in the bulk sample.

ceptibility of the oxygen-annealed samples was found to be independent of temperature down to 78 K. Curve (b) in Fig. 2 shows the temperature dependence of the resistivity of the same sample. The zero-resistance temperature of the nitrogen-annealed sample was found to be 91 K, but after annealing in oxygen the zero-resistance temperature fell to below 78 K. Subsequent annealing in nitrogen was found to restore the zero-resistance temperature to 91 K. Similar results were found for all of our samples.

X-ray diffraction was carried out at room temperature with nickel-filtered Cu *Kd* radiation on a Philips wide-angle goniometer. X-ray-diffraction patterns of a typical sample after annealing in oxygen and after annealing in nitrogen show no evidence of a second phase or of the presence of unreacted materials. Most of the diffraction lines shift to higher angles after annealing the sample in nitrogen. The shift can be reversed by subsequently annealing in oxygen. Our best estimates of the lattice parameters deduced from the x-ray-diffraction data are reported in Table I. Our results, which indicate that for $Bi_2CaSr_2Cu_2O_{8+\delta}$ the lattice parameter a stays essentially constant and c increases as the oxygen content decreases, are consistent with the observations of other workers.[20,21]

In order to check for the presence of disordered impurity phases and unreacted constituents, which might not show up in the x-ray-diffraction pattern, the microstructures of the nitrogen- and oxygen-annealed samples were analyzed by means of a Hitachi 5-570 scanning electron

TABLE I. Lattice parameters measured at room temperature for bismuth 2:1:2:2 samples annealed in nitrogen and oxygen. The lattice parameters are based on an assumed tetragonal unit cell.

	Nitrogen annealed	Oxygen annealed
a	3.813	3.810
c	30.773	30.675
$T_{R=0}$	90–94 K	$\leq$78 K

microscope (SEM) equipped with a Kovex H-800 energy-dispersive x ray (EDX) attachment. The SEM results show the presence of voids with a total area of approximately 10% of the area of each sample, as well as small inclusions of a dark phase with a total area of less than 2%. EDX analysis confirms that the predominant phase corresponds to the 2:1:2:2 superconducting phase, and that the dark phase is a bismuth-deficient phase. The present samples are very homogeneous and very dense, with a grain size in the range 1–5 μm.

The micrographs reveal no obvious difference between the nitrogen- and oxygen-annealed samples, indicating that annealing at 500 °C (which is well below the melting temperature of 870 °C) does not alter the average structure of the cations. Therefore, the principal effect of annealing at 500 °C in an oxygen-reduced atmosphere will be to remove oxygen from the lattice, and the principal effect of annealing in oxygen gas will be to restore it.

III. RESULTS AND DISCUSSION

In order to search for evidence of changes in the distribution of oxygen atoms brought about by annealing, Raman scattering measurements have been carried out at normal incidence in a back-scattering geometry using a Spex 1877B Raman spectrometer. The excitation radiation was the 514.5-nm (19 436-cm^{-1}) line of an argon-ion laser operating in the TEM_{00} mode. The diameter of the diffraction-limited focal spot was estimated to be 6.8 μm.

Preliminary experiments comparing the Raman spectra of a single sample of bismuth 2:1:2:2 after annealing for 24 h at 500 °C in oxygen and nitrogen gas showed that the removal of oxygen brought about a significant increase in the intensity of the oxygen peak at 650 cm^{-1}, while the intensities of the other oxygen peaks were unchanged. To verify this unexpected result, laser annealing techniques were adopted to study the temperature dependences of the various oxygen peaks.

Each sample was annealed in an external oven in an atmosphere of pure oxygen gas at 500 °C, then mounted in the sample holder of the Raman spectrometer in an atmosphere of air. With low power in the laser beam, the beam was focused on the sample and the position of the focal spot was adjusted until the strongest Raman scattering was obtained. The power in the laser beam was increased in steps to a maximum well below the power required to melt the sample and then decreased in

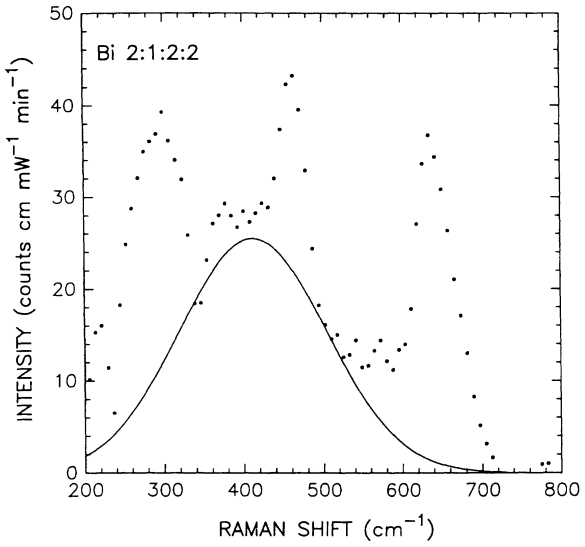

FIG. 3. Raman spectrum of a sintered sample of bismuth 2:1:2:2. The temperature of the illuminated region of the sample is 440 °C. The tail of the Rayleigh scattering peak has been subtracted. The data show a broad background peak, which is believed to be of electronic origin. The solid curve is our best Gaussian approximation to the background peak.

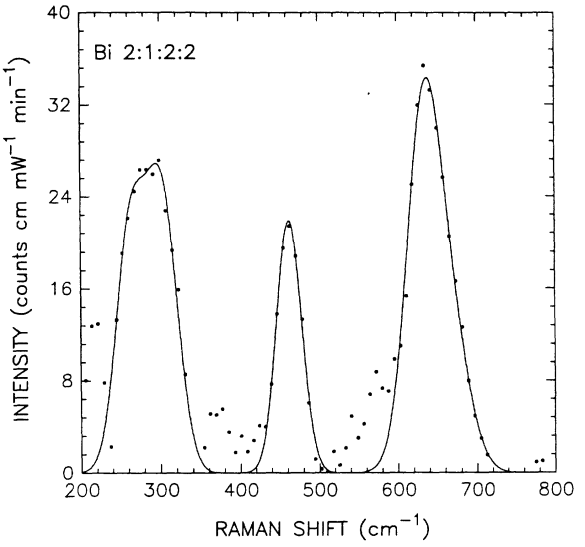

FIG. 4. The vibrational Raman spectrum of a sintered sample of bismuth 2:1:2:2. The data are the same as in Fig. 3, but the background peak has been subtracted off.

steps to zero. The cycle of heating and cooling was then repeated. The Stokes spectrum was recorded at every step. By analyzing the resulting spectra, irreversible effects due to oxygen depletion can be distinguished from reversible effects due to thermal expansion.

Strong Rayleigh scattering restricts the measured distributions to frequency shifts greater than about 200 cm^{-1}. Figure 3 shows the Raman spectrum of a typical sample after correction to remove the residual Rayleigh background. Prominent vibrational peaks occur in the vicinity of 300, 470, and 650 cm^{-1}. There is a well-defined peak near 210 cm^{-1}, while the peak near 300 cm^{-1} appears to be a poorly resolved triplet. In some of our samples the upper peaks are accompanied by shoulders that may represent weaker peaks in the vicinity of 410 and 625 cm^{-1}. There is also a broad background peak that is believed to be of electronic origin.

Once the laser-annealing data had been completed, the temperature rise of the illuminated region of the sample was determined as a function of the power in the laser beam by measuring the intensities of the Stokes and anti-Stokes spectra and correcting for effects due to the photon-induced departure from thermodynamic equilibrium. The calibration technique has been described in detail elsewhere.[16]

Measurements on many samples show that the broad background peak can be represented to a good approximation by a Gaussian distribution. Therefore, the vibrational Raman spectrum was extracted from the data by subtracting a Gaussian distribution fit to the background. The resulting spectrum is shown in Fig. 4. The intensities of the principal vibrational modes were determined by fitting the corrected spectrum with distributions of

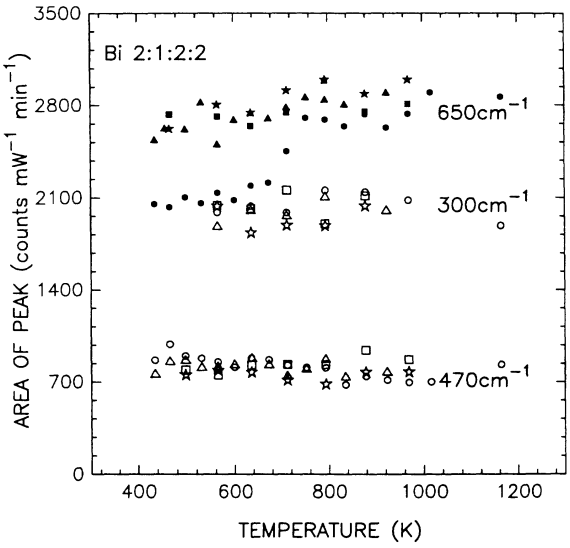

FIG. 5. Intensities of the three prominent oxygen peaks in the Raman spectrum of sintered bismuth 2:1:2:2, corrected for varying laser beam intensity and plotted as a function of the temperature of the illuminated region of the sample. Circles denote the first sweep with increasing temperature, triangles denote the first sweep with decreasing temperature, squares denote the second sweep with increasing temperature, and stars denote the second sweep with decreasing temperature. The data show weak reversible temperature dependences that are presumably caused by thermal expansion. The 650-cm^{-1} peak alone shows an irreversible change in the vicinity of 500 °C, which is attributed to loss of oxygen from the bismuth layer.

gaussian form. In Fig. 5 the intensities, normalized to unit power in the laser beam, are plotted as a function of the temperature of the illuminated region of the sample. In the temperature range from 290 to 1100 K, only the shoulder and peak near 650 cm^{-1} are significantly affected by annealing in an oxygen-reduced atmosphere. The increase in the strength of this peak (normalized to unit power in the laser beam) is conserved if the power in the laser beam is subsequently reduced, but it can be reversed by annealing the sample in dry oxygen gas at 500 °C. The normalized intensities of the other oxygen peaks are unchanged up to the melting temperature.

As the temperature rises, the Raman shifts of all of the oxygen peaks decrease. Data for the 470 and 650 cm^{-1} peaks, plotted in Figs. 6 and 7, suggest that the slopes of the temperature dependences of the Raman shifts change in the vicinity of 700 K. However, there is no indication of irreversibility in the temperature range 640 to 760 K, over which loss of oxygen occurs in the first cycle of laser heating. Therefore, the increase in the intensity of the 650 cm^{-1} peak that is caused by deoxygenation is not accompanied by any perceptible change in Raman shift.

If it is assumed, on the basis of the evidence described above, that the shoulder and peak near 650 cm^{-1} arise from oxygen atoms in the bismuth layer, then the observation that the intensity of this peak alone changes irreversibly is evidence that in bismuth 2:1:2:2 the mobile oxygen sites lie in the bismuth layer. If deoxygenation involves the loss of oxygen atoms that contribute to the 650 cm^{-1} Raman peak, then its intensity would be expected to decrease. The unexpected finding that deoxygenation increases the strength of the 650 cm^{-1} peak without changing its frequency, may be a clue to the oxygen structure of the bismuth layer.

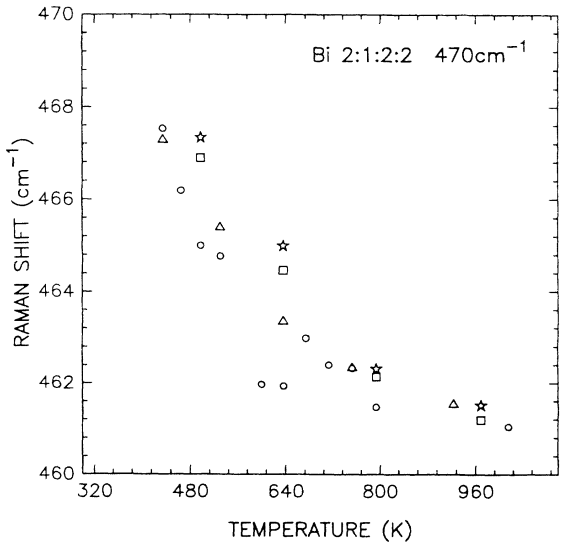

FIG. 6. The temperature dependence of the center of the 470-cm^{-1} Raman peak for bismuth 2:1:2:2. The successive sweeps are denoted as in Fig. 5. The data suggest a reversible change of slope in the vicinity of 700 K but show no irreversible behavior.

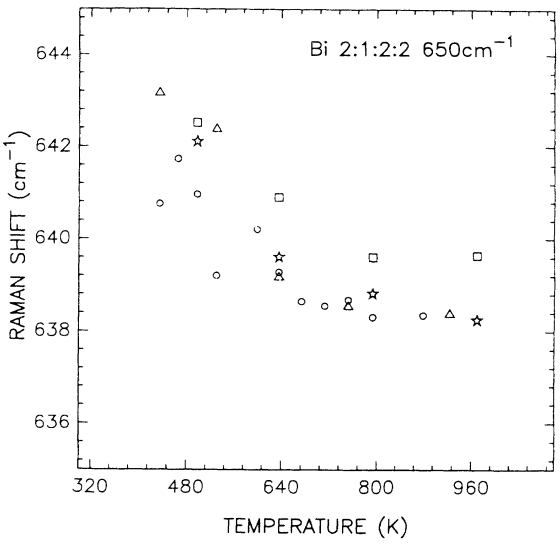

FIG. 7. The temperature dependence of the center of the 650-cm^{-1} Raman peak for bismuth 2:1:2:2. The successive sweeps are denoted as in Fig. 5. The data suggest a reversible change of slope in the vicinity of 700 K but show no irreversible behavior in the temperature range 640–760 K, over which an irreversible increase in the peak intensity is observed.

There is one oxygen atom per bismuth atom in the limit $\delta=0$ (i.e., O_8), and there are two oxygen atoms per bismuth atom in the limit $\delta=2$ (i.e., O_{10}). Various models of oxygenation have been proposed in which oxygen is incorporated by the progressive occupation of the vacant sites in the BiO layers until the BiO_2 structure is achieved. Bordet *et al.*[4] have proposed that in the limit $\delta=0$ the oxygen atoms are close to, but offset from, the centers of the squares defined by the bismuth atoms, the atoms being distributed over the four equivalent sites in a disordered array. von Schnering *et al.*[5] have suggested an alternative model in which the bismuth atoms form a square lattice and the oxygen sites are located midway between nearest-neighbor bismuth atoms. In the limit $\delta=2$, the oxygen sites are fully occupied, while in the limit $\delta=0$, the oxygen atoms occupy one half of the oxygen sites in an ordered arrangement, which conforms to the space group *Amaa*. Studies of convergent beam electron diffraction by Withers *et al.*[6] led Bordet *et al.*[7] to refine the neutron data in the noncentric space group *A2aa*, on the basis of which they proposed a further revised model for the limit $\delta=0$ in which the oxygen atoms are distributed in an ordered array over sites offset from the centers of the bismuth squares.

More recent data indicate that excess oxygen in bismuth 2:1:2:2 is incorporated interstitially. Electron diffraction experiments[8] have revealed an incommensurate structural modulation in the *a* direction, whose average spatial periodicity (typically 4.7 times the cell dimension) depends on the conditions of sample preparation. Hewat *et al.*[22] have proposed a model for the incorporation of excess oxygen in $Bi_2CaSr_2Cu_2O_8$ that offers a con-

sistent interpretation of the diffraction data and the results of high-resolution electron microscope imaging. In Hewat's model, the excess oxygen is incorporated interstitially in the BiO layers by inserting oxygen atoms between adjacent bismuth atoms in planes normal to the *a* axis. Relaxation of the structure due to the incorporation of excess oxygen leads to canting of the perovskite columns and periodic modulation of the BiO layers, which is consistent with electron microscope images observed in [010] projection.

Beshrovnyi *et al.*[10] have carried out refinements of single-crystal neutron-diffraction data for $Bi_2CaSr_2Cu_2O_8$ based on a large supercell. Their results indicate a modulation in the *a* direction that is due to the insertion of an oxygen atom in an interstitial site between adjacent bismuth atoms in every fifth subcell. The oxygen superlattice in the bismuth layer causes a flexing of the structure, which greatly resembles that described by Hewat *et al.* Similar results have been reported for materials apparently isostructural with the bismuth oxide superconductors.[23]

The observed increase in the intensity of the 650-cm^{-1} Raman peak on deoxygenation, without any perceptible change in its Raman shift, is difficult to understand on the basis of models in which excess oxygen is incorporated on a lattice, but it is consistent with models in which excess oxygen is incorporated interstitially. The 650-cm^{-1} Raman peak represents the vibrations of oxygen atoms associated with the BiO lattice, while, according to these models, deoxygenation involves the loss of excess oxygen from interstitial sites. Raman peaks corresponding to oxygen atoms in interstitial sites have not been detected. However, interstitial oxygen might affect the Raman spectrum indirectly by lowering the symmetry around a fraction of the BiO lattice groups. Deoxygenation causes the symmetry to be restored, increasing the intensity of the 650-cm^{-1} Raman peak. Alternative models based on the perturbation of the vibrational modes of the lattice by interstitial oxygen appear to be inconsistent with our finding that deoxygenation causes no perceptible change in the Raman shift.

According to Hewat's model, the spatial periodicity of the superlattice in the *a* direction represents the average distance between the planes of interstitial oxygen atoms. Hence the spatial periodicity of the superlattice is expected to increase as the amount of excess oxygen decreases. High-resolution electron-diffraction studies by Li and coworkers[11,12] have shown that the spatial periodicity of the modulation increases progressively as the sample is heated in a vacuum and that the incommensurate structure vanishes in the vicinity of 500 °C. The irreversible increase observed over the same temperature range in the intensity of the Raman peak, which corresponds to oxygen atoms in the bismuth layer, strongly suggests that the incommensurate-to-commensurate phase transition is due to loss of oxygen from the bismuth layer of the vacuum-annealed sample.

Further support for a link between the oxygen content of the bismuth layer and the spatial periodicity of the superlattice comes from experiments in which partial replacement of Sr^{2+} by La^{3+} is found to reduce the average periodicity of 3.4 times the cell dimension.[9] Since the preservation of charge neutrality requires that the substitution of divalent strontium by trivalent lanthanum be accompanied by the incorporation of extra oxygen, a possible interpretation is that the increase in oxygen content is responsible for the observed decrease in the spatial periodicity of the superlattice. Interpreted in this way, the lanthanum substitution experiments are also consistent with our interpretation of the Raman data.

In our materials, the removal of oxygen brings about significant increases in the superconducting transition temperature, the normal-state resistivity, and the *c* lattice parameter. Whereas our oxygen-reduced samples were prepared in air, and our measurements did not extend below 78 K, Groen and de Leeuw[21] have reported that the transition temperature of bismuth 2:1:2:2 can be depressed by as much as 40 K by annealing the sample in an atmosphere with a sufficiently low partial pressure of oxygen, and that an unambiguous relationship between T_c, *c*, and degree of oxygenation exists over a very wide range of oxygen partial pressure.

A striking feature of the data is that a very small change in oxygen content is sufficient to bring about large changes in T_c and in the *c* lattice parameter. It is interesting to speculate on the underlying mechanism. Oxygen is incorporated in the bismuth layers as negative ions, the accompanying holes being distributed among the various layers. Thus oxygenation has the effect of extrinsically doping the CuO layers. Though superconductivity in the oxide superconductors is widely associated with the presence of holes in the CuO layers, Groen and de Leeuw[21] find that the change in hole density associated with deoxygenation is far too small to account for the observed change in T_c. The present data show that deoxygenation brings about both an increase in the superconducting transition temperature, which might be associated with an increase in the hole density, and also an increase in the normal-state resistivity, which might be associated with a decrease in the hole density. This inconsistency is further evidence that the increase in T_c associated with deoxygenation is not caused primarily by the change in extrinsic doping.

Electronic band-structure calculations[24–26] show that in the vicinity of the Fermi level the energy bands of the CuO layer are slightly overlapped by bands of the BiO layers. The result is that, in the stoichiometric material, the CuO bands are doped intrinsically by the BiO layers with about 0.1 holes per copper atom. The incorporation of excess oxygen is known to induce a flexing of the BiO layers, as well as a contraction in the *c* direction. In the absence of detailed calculation it is impossible to predict with any assurance the consequences of these structural changes. If the effect were to raise the energy of the bottom of the BiO band relative to the Fermi level, then oxygenation would reduce the intrinsic doping of the CuO layer. This would tend to suppress the superconducting transition, in agreement with experimental studies of bismuth 2:1:2:2. It is interesting to note that, in thallium 2:1:2:2:, T_c is reduced by annealing in an oxygen-reduced environment.[27] That such similar materials respond to oxygenation in very different ways suggests that the ob-

served behavior may be governed by subtle features of the response of the electronic structure to oxygen-induced structural changes.

IV. CONCLUSIONS

The zero-resistance temperatures of sintered samples of the oxide superconductor $Bi_2CaSr_2Cu_2O_{8+\delta}$ can be raised to above 90 K by annealing at 500 K in an oxygen-reduced atmosphere. Raman studies show that the intensity of the 650-cm^{-1} peak is significantly increased by annealing in an oxygen-reduced atmosphere, and that the effect can be reversed by annealing in oxygen, while the intensities of the other prominent oxygen peaks are unchanged. Deoxygenation causes no perceptible change in the Raman shift of any of the oxygen peaks. These findings confirm that the 650-cm^{-1} peak is associated with normal modes that are dominated by the motions of oxygen atoms in the BiO layer. That loss of oxygen should bring about an increase in the intensity of this Raman peak alone, the Raman shift remaining constant, is consistent with those models of the oxygen structure in which excess oxygen is incorporated interstitially. The Raman data indicate that loss of oxygen occurs in the same temperature range as the incommensurate-to-commensurate phase transition that has been observed in electron diffraction, suggesting that the phase transition is caused by loss of oxygen from the bismuth layer due to annealing in the vacuum chamber of the electron microscope. Band-structure calculations indicate that the CuO layers in bismuth 2:1:2:2 are doped intrinsically by the BiO layers. It is suggested that the striking sensitivity of T_c to the presence of excess oxygen may be due to changes in the intrinsic doping of the CuO layers brought about by oxygen-induced changes in the structure of the BiO layers.

ACKNOWLEDGMENTS

We are indebted to Z. X. Zhou and J. V. Yakhmi for stimulating discussions, and to J. Rutter and S. Bagheri for help with SEM sample characterization. This work was carried out using the Raman facilities of the Ontario Laser and Lightwave Centre, and was supported in part by a grant from the Natural Sciences and Engineering Research Council of Canada.

[1]H. Maeda, Y. Tanaka, M. Fukutomi, and T. Asano, Jpn. J. Appl. Phys. **27**, L209 (1988).

[2]A. Maeda, M. Hase, I. Tsukada, K. Noda, S. Takebayashi, and K. Uchinokura, Phys. Rev. B **41**, 6418 (1990).

[3]P. V. P. S. S. Sastry, I. K. Gopalakrishnan, A. Sequira, H. Rajagopal, K. Gangadharan, G. M. Phatak, and R. M. Iyer, Physica C **156**, 230 (1988).

[4]P. Bordet, J. J. Capponi, C. Chaillout, J. Chenavas, A. W. Hewat, E. A. Hewat, J. L. Hodeau, M. Marezio, J. L. Thoulence, and D. Tranqui, Physica C **153-155**, 623 (1988).

[5]H. G. von Schnering, L. Walz, M. Schwarz, W. Becker, M. Hartweg, T. Popp, B. Hettich, P. Müller, and G. Kämph, Angew. Chem. Int. Ed. Engl. **27**, 574 (1988).

[6]R. L. Withers, J. S. Anderson, B. G. Hyde, J. G. Thompson, L. R. Wallenberg, J. D. Fitzgerald, and A. M. Steward, J. Phys. C **21**, L417 (1988).

[7]P. Bordet, J. J. Capponi, C. Chaillout, J. Chenavas, A. W. Hewat, E. A. Hewat, J. L. Hodeau, M. Marezio, J. L. Thoulence, and D. Tranqui, Physica C **156**, 189 (1988).

[8]M. Onoda, A. Yamamoto, E. Takayama-Muromachi, and S. Takekawa, Jpn. J. Appl. Phys. **27**, L833 (1988).

[9]W. W. Zandbergen, W. A. Groen, F. C. Mijlhoff, G. van Tendeloo, and S. Amelinckx, Physica C **156**, 325 (1988).

[10]A. I. Beskrovnyi, M. Dlouha, Z. Jirak, S. Vratislav, and E. Pollert, Physica C **166**, 79 (1990).

[11]C. Chen, J. Q. Li, Y. S. Yao, X. M. Huang, Z. X. Zhao, and W. K. Wang, Solid State Commun. **68**, 749 (1988).

[12]J. Q. Li, C. Chen, D. Y. Yang, F. H. Li, Y. S. Yao, Z. Y. Ran, W. K. Wang, and Z. X. Zhao, Z. Phys. B **74**, 165 (1989).

[13]J. Prade, A. D. Kulkarni, F. W. de Wette, U. Schroder, and W. Kress, Phys. Rev. B **39**, 2771 (1989).

[14]J. M. Tarascon, Y. Le Page, P. Barboux, B. G. Bagley, L. H. Green, W. R. McKinnon, G. W. Hull, M. Giroud, and D. M. Hwang, Phys. Rev. B **37**, 9382 (1988).

[15]M. Cardona, C. Thomsen, R. Liu, H. G. von Schnering, M. Hartweg, Y. F. Fan, and Z. X. Zhao, Solid State Commun. **66**, 1225 (1988).

[15a]M. Boekholt, A. Erle, P. C. Splittgerber-Hünnekes, and G. Güntherodt, Solid State Commun. **74**, 1107 (1990).

[16]Y. H. Shi, M. J. G. Lee, M. Moskovits, A. Hsu, and R. Carpick, J. Appl. Phys. **70**, 1915 (1991).

[17]R. G. Buckley, J. T. Tallon, I. W. M. Brown, M. R. Presland, P. W. Gilbert, M. Bowden, and N. B. Milestone, Physica C **156**, 629 (1988).

[18]J. Zhao and M. S. Seehra, Physica C **159**, 639 (1989).

[19]N. H. Wang, C. M. Wang, H.-C. I. Kao, D. C. Ling, H. C. Ku, and K. H. Lii, Jpn. J. Appl. Phys. **28**, L1505 (1989).

[20]H. Niu, N. Fukushima, K. Takenchi, and K. Ando, Jpn. J. Appl. Phys. **27**, L1442 (1988).

[21]W. A. Groen and D. M. de Leeuw, Physica C **159**, 417 (1989).

[22]E. A. Hewat, J. J. Capponi, and M. Marezio, Physica C **157**, 502 (1989).

[23]Y. Le Page, W. R. McKinnon, J.-M. Tarascon, and P. Barboux, Phys. Rev. B **40**, 6810 (1989).

[24]M. S. Hybertson and L. F. Mattheiss, Phys. Rev. Lett. **60**, 1661 (1988).

[25]L. F. Mattheiss and D. R. Hamann. Phys. Rev. B **38**, 5012 (1988).

[26]S. Massida, J. Yu, and A. J. Freeman, Physica C **152**, 251 (1988).

[27]I. K. Gopalakrishnan, P. V. P. S. S. Sastry, K. Gangadharan, G. M. Phatak, J. V. Yakhmi, and R. M. Iyer, Appl. Phys. Lett. **53**, 414 (1988).